

Modeling of Kinetic Interface Sensitive Tracers for Two Phase Immiscible Flow in Porous Media with COMSOL Multiphysics

Alexandru-Bogdan Tatomir^{*1}, Apoorv Jyoti¹, Friedrich Maier¹ and Martin Sauter¹

¹Dept. of Applied Geology, Geoscience Centre of the University of Göttingen

^{*}Corresponding author: Goldschmidtstr. 3, 37077, Göttingen, Germany, alexandru.tatomir@geo.uni-goettingen.de

Abstract: The understanding of the tracer migration in two-phase porous media systems and its reaction over the fluid-fluid interfaces is a challenging task important for a number of engineering applications, e.g. oil recovery, carbon capture and storage in geological reservoirs, remediation groundwater contaminations, etc.

The goal of this work is to implement in COMSOL Multiphysics an immiscible two-phase flow and tracer transport, accounting for the fluid-fluid interfacial area and a hydrolysis reaction over the interface.

The pressure-saturation formulation is chosen among two-phase flow formulations. For closing the system of equations a relationship based on Brooks-Corey approach among capillary pressure, saturation and interfacial area formulation is used. The strongly coupled, parabolic system of partial differential equations is build using the coefficient form PDE interface. The hydrolysis of tracer at the fluid-fluid interfaces follows a pseudo-zero order kinetic reaction and it is implemented with the solute transport interface.

Keywords: two-phase flow, reactive transport, porous media, kinetic interface sensitive tracer, CO₂

1. Introduction

Tracer testing are powerful methods for characterization and for understanding the processes occurring in geologic reservoirs. Kinetic Interface Sensitive (KIS) tracer concept has been developed with the intention to estimate the amount of interface between two fluid phases. One direct application is monitoring the spreading of injected supercritical CO₂ in geological formations (Schaffer et al. 2013).

The KIS tracer is injected dissolved in the non-wetting phase and undergoes a hydrolysis reaction over the interface resulting in an alcohol and an acid dissolved in the wetting phase. Both alcohol and acid are only present in the wetting phase and there is negligible back partitioning. For the

monitoring purposes it is sufficient to track only the acid (tracer) which can indicate the amount of interfacial area between the two fluids.

This article describes the implementation in the COMSOL Multiphysics (version 4.4) framework of the mathematical model of two phase immiscible flow and a tracer transport in porous media, first introduced in (Tatomir et al. 2013)

Two numerical simulations for two different spatial-scales are shown as examples.

The model is tested with respect to the sensitivity of different flow and transport parameters (e.g., permeability, porosity, reaction rate, injection rate).

2. Mathematical Model for Two-Phase Flow and KIS Tracer Transport in Porous Media

2.1 Two-Phase Flow in Porous Media

The mathematical model describing immiscible two-phase flow in porous media is based on the extended Darcy's law and can be written as (Helmig 1997):

$$\frac{\partial(S_{\alpha}\phi\rho_{\alpha})}{\partial t} - \nabla \cdot \left(\frac{\rho_{\alpha}\mathbf{K}k_{r\alpha}}{\mu_{\alpha}} (\nabla p_{\alpha} - \rho_{\alpha}\mathbf{g}) \right) - \rho_{\alpha}q_{\alpha} = 0 \quad (1)$$

All parameters are defined in Table 2 (Nomenclature).

The classical coupling relations are:

$$S_w + S_n = 1 \quad (2)$$

$$p_n - p_w = p_c(S_w) \quad (3)$$

The interfacial area between the two fluid phases can be expressed averaged on an REV with a relationship (Tatomir et al. 2013):

$$a_{wn}(S_w, p_c) = a_0 \cdot (S_w)^{a1} \cdot (1 - S_w)^{a2} \cdot (p_c^{max} - p_c)^{a3} \quad (4)$$

The “a_i” coefficients can be determined from pore-scale simulations (Joekar-Niasar et al. 2008).

The constitutive relationship between capillary pressure and saturation is formulated using Brooks-Corey model:

$$p_c(S_w) = p_d \cdot S_e^{-\frac{1}{\lambda}} \text{ with } S_e = \frac{S_w - S_{wr}}{1 - S_{wr}} \quad (5)$$

and for relative permeability using a Burdine-Brooks-Corey approach:

$$k_{rw} = S_e^{\frac{2+3\lambda}{\lambda}}, \quad k_{rn} = (1 - S_e)^2 \cdot \left(1 - S_e^{\frac{2+\lambda}{\lambda}}\right) = 0. \quad (6)$$

The pressure-saturation formulation is chosen among two-phase flow formulation because it has the most advantages (Helmig 1997). Wetting pressure and non-wetting saturations are the two primary variables.

2.2 Acid Tracer Transport

It is assumed that the KIS tracer is completely dissolved in the non-wetting phase and that there is in sufficient quantity such that the fluid-fluid interfaces will always remain saturated. KIS tracer's reaction products are acid and alcohol. For the quantification of the interfacial area it is only necessary to add the transport equation for the acid byproduct. Therefore, the solute transport equation for acid concentration C is:

$$\phi \frac{\partial C}{\partial t} - \nabla \cdot (Cv_w - \phi D \nabla C) - q_{n \rightarrow w}^R = 0 \quad (7)$$

The hydrolysis reaction is represented averaged over the entire elementary volume by an effective specific interfacial area term and an effective rate coefficient. It is assumed that the reaction follows a zero order kinetic law:

$$q_{n \rightarrow w}^R = k_{n \rightarrow w}^R a_{wn} \quad (8)$$

3. Model Implementation in COMSOL Multiphysics

The model implementation consists of two parts. The first one is the immiscible two-phase flow in porous media and the second is the KIS tracer transport in the wetting phase.

3.1 Immiscible Two-Phase Flow in Porous Media Model Implementation

The implementation of the two-phase immiscible fluid model is done within the Coefficient Form PDE (Partial Differential Equation) interface.

The two-phase flow equation (1) is written for each phase having p_w, S_n as primary variables:

$$-\frac{\partial(S_n \phi \rho_w)}{\partial t} - \nabla \cdot \left(\frac{\rho_w \mathbf{K} k_{rw}}{\mu_w} (\nabla p_w - \rho_w \mathbf{g}) \right) - \rho_w q_w = 0 \quad (9)$$

$$\frac{\partial(S_n \phi \rho_n)}{\partial t} - \nabla \cdot \left(\frac{\rho_n \mathbf{K} k_{rn}}{\mu_n} (\nabla p_w + \nabla p_c - \rho_n \mathbf{g}) \right) - \rho_n q_n = 0 \quad (10)$$

COMSOL requires a transformation of variables with respect to p_w and S_n . The chain rule formula in calculus allows us to write:

$$\nabla p_c = \frac{dp_c}{dS_n} \nabla S_n \quad (11)$$

In COMSOL the Coefficient Form PDE equation for the primary variable \mathbf{u} has the following expression:

$$e_a \frac{\partial^2 \mathbf{u}}{\partial^2 t} + d_a \frac{\partial \mathbf{u}}{\partial t} + \nabla \cdot (-c \nabla \mathbf{u} - \alpha \mathbf{u} + \gamma) + \beta \cdot \nabla \mathbf{u} + \mathbf{a} \mathbf{u} = f \quad (12)$$

The two primary variables are:

$$\mathbf{u} = \begin{pmatrix} p_w \\ S_n \end{pmatrix} \quad (13)$$

Next the PDE coefficients are introduced:

$$d_a = \begin{pmatrix} 0 & -\phi \rho_w \\ 0 & \phi \rho_n \end{pmatrix} \quad (14)$$

$$c = \begin{pmatrix} K \lambda_w \rho_w & 0 \\ K \lambda_n \rho_n & K \lambda_n \rho_n \left(\frac{dp_c}{dS_n} \right) \end{pmatrix} \quad (15)$$

From equation (5) the derivative can be written:

$$\frac{dp_c}{dS_n} = \frac{1}{\lambda} \cdot p_d \cdot (1 - S_n)^{\left(-\frac{1}{\lambda}-1\right)} \quad (16)$$

3.2 KIS Tracer Transport in Wetting Phase Model Implementation

For the implementation of the KIS tracer transport in the wetting phase in porous media the ‘‘Solute Transport’’ module is used. The number of species in the system is set to 1 and the concentration is assigned the symbol c .

Two couplings between the PDE module and solute transport module were enabled. First the solution for the flow velocity of the wetting fluid, as carrier fluid, from the PDE module is specified as user defined velocity in the Solute Transport module. Second, a reaction node is added to define the hydrolysis of the KIS tracer over the fluid-fluid interface (Eq. (8)). In doing so, the specific interfacial area, a_{wn} is coupled with the S_n from PDE module defined in Eq. (4).

4. Numerical Simulations

4.1 Laboratory Core-scale Column Experiment

The first simulated numerical example is a 2D horizontal laboratory column with the dimensions of 50cm x 3cm (Figure 12a). For this quasi one-dimensional case, the gravity term is neglected. The non-wetting phase is injected together with KIS tracer on the left side of the domain at a constant rate of $1.0e-3 \text{ kg/m}^2\cdot\text{s}$ for 1 day. This is specified as a “Flux/source” node in the “Coefficient Form PDE” module. For solute transport the left boundary is initialized with a zero concentration. The acid tracer concentration is produced in the domain when the saturations are not zero as a source term. On the right side of the column the boundary condition is defined as Dirichlet with constant non-wetting phase saturation 0.0, and a wetting pressure of 1 bar; as for the tracer transport, the right boundary is set as outflow. On upper and lower boundaries we set no-flow boundary conditions. The initial conditions are 1 bar for the wetting pressure, 0.0 for the non-wetting saturation, and 0 g/l tracer concentration. The initial values specified in Table 1 are kept constant throughout the domain.

4.2 Field-scale Single-Well Injection Experiment

The second numerical example is that of a single well (field scale) injection. Because the domain is homogeneous and symmetric only a quarter needs to be solved, therefore the dimensions of the simulated domain are 100m x 80m (Figure 12b). The non-wetting phase is injected at the lower left corner of the domain with the distributed rate of $0.01 \text{ kg/m}^2\cdot\text{s}$ for 30 days.

The boundary conditions are set no flow on lower and left sides, and Dirichlet ($p_w = 100 \text{ bar}$ and $S_n = 0$) elsewhere.

5. Results and discussions

5.1 Laboratory Scale Results

The sensitivity analysis with respect to the effective porosity of the system is depicted in figures 1 to 3 in the form of breakthrough curves (BTCs) of acid concentration, non-wetting saturation and specific interfacial areas. The center of the column is chosen as observation point for plotting the results. The porosity was varied from a very less porous system 10% to a highly porous system with a porosity of 30%.

It can be observed that the change in porosity is affecting the front speed, which is the expected behavior. The front is fastest for the least porous value in the system i.e. 10%. This behavior can also be seen in the acid concentration BTC.

Next we perform a sensitivity analysis to investigate the effect of the non-wetting phase injection rate on breakthrough curves of acid concentration, non-wetting saturation and specific interfacial area. The injection rate is varied from $7.e-4$ to $2.5e-3 \text{ kg/m}^2\cdot\text{s}$. The results are plotted in Figure 4, Figure 5 and Figure 6.

Figure 7 illustrates the tracer concentration BTCs for different reaction rates at center of the column. We can observe that a higher reaction rates lead as expected to higher concentrations. Nevertheless, some results are out of the physical range as the KIS tracer is never depleted at the interface and acid is produced as long as both phases are present (saturation is neither zero or one).

5.2 Field Scale Results

For Field Scale evaluation we implement a sensitivity analysis of two main parameters, the porosity of the system (ϕ) and the reaction rate ($k_{n \rightarrow w}^R$).

Similarly to the laboratory-scale example the results are illustrated in the form of BTCs of acid concentration, non-wetting saturation and specific interfacial areas.

The sensitivity analysis with respect to changing porosity of the system (from 10% to highly porous material of 40%) is given in Figure 8 (specific interfacial area), Figure 9 (non-wetting saturation) and Figure 10 (tracer concentration).

We can conclude that by increasing the porosity of the system non-wetting saturation front is being slowed, as well as, the movement of the interface and that of the tracer concentration. The less porous is the system, the interface moves faster in the domain and reaches higher peak-concentrations (Figure 10). On the contrary, the peak saturation and specific interfacial area is not affected by porosity (Figure 8, Figure 9).

The sensitivity analysis with respect to the reaction rate of KIS tracer over the wetting-non-wetting interface is illustrated in Figure 11. The rate is varied between $1 \cdot e^{-4}$ and $1 \cdot e^{-6}$ $\text{kg/m}^2 \cdot \text{s}$.

6. Summary and Conclusions

We have introduced a mathematical model for KIS tracer transport in two-phase immiscible flow in porous media. Next we have introduced the steps for the model implementation into COMSOL Multiphysics version 4.4.

Two porous media systems, at laboratory- and field-scale have been shown as numerical examples. Several sensitivity studies have investigated the behavior of the tracer concentration, the interfacial area and fluid saturation, with regard to several flow and transport parameters. The simulation results help us gain a better understanding on the behavior of one of KIS tracer's reaction product.

Last but not least, COMSOL provides a good environment to implement and simulate two-phase flow and tracer transport accounting for fluid-fluid interfacial area.

7. References

1. Helmig, R., *Multiphase Flow and Transport Processes in the Subsurface: A Contribution to the Modeling of Hydrosystems 1st ed.*, Springer, (1997)
2. Joekar-Niasar, V. et al., Insights into the Relationships Among Capillary Pressure, Saturation, Interfacial Area and Relative Permeability Using Pore-Network Modeling. *Transport in Porous Media*, 74(2), pp.201–219 (2008)
3. Schaffer, M. et al., A new generation of tracers for the characterization of interfacial areas during supercritical carbon dioxide injections into deep saline aquifers: Kinetic interface-sensitive tracers (KIS tracer). *International Journal of Greenhouse Gas Control*, 14, pp.200–208 (2013)

4. Tatomir, A. et al., Modelling of Kinetic Interface Sensitive Tracers for Two-Phase Systems. In M. Z. Hou, H. Xie, & P. Were, eds. *Clean Energy Systems in the Subsurface: Production, Storage and Conversion*. Springer Series in Geomechanics and Geoengineering, Springer Berlin Heidelberg, pp. 65–74 (2013)

8. Acknowledgements

This research has received funding from the European Community's 7th Framework Programme through the MUSTANG (Grant agreement no. 227286) and TRUST (Grant agreement no. 309067) projects.

9. Appendix

Table 1: The initial values used for the two numerical examples

Parameter	Laboratory Scale values	Field Scale values
ϕ	0.2	0.2
k	$1 \cdot e^{-12}$ [m^2]	$1 \cdot e^{-10}$ [m^2]
ρ_w	1000 [kg/m^3]	1000 [kg/m^3]
ρ_n	700 [kg/m^3]	700 [kg/m^3]
λ	2	2
p_d	2000[Pa]	2000[Pa]
P_w	10^5 [Pa]	10^7 [Pa]
S_n	0.0	0.0
Q_{in}	$1.0 \cdot e^{-4}$ [$\text{kg/m}^2 \cdot \text{s}$]	$1.0 \cdot e^{-3}$ [$\text{kg/m}^2 \cdot \text{s}$]
μ_n	$1.0 \cdot e^{-4}$ [Pa·s]	$1.0 \cdot e^{-4}$ [Pa·s]
μ_w	$1.0 \cdot e^{-3}$ [Pa·s]	$1.0 \cdot e^{-3}$ [Pa·s]
$k_{n \rightarrow w}^R$	$1.0 \cdot e^{-6}$ [$\text{kg/m}^2 \cdot \text{s}$]	$1.0 \cdot e^{-6}$

Table 2: Nomenclature

ρ_w	Density of Wetting Phase
μ_w	Viscosity of Wetting Phase
K	Intrinsic Permeability
ϕ	Porosity (phi)
S_n	Saturation of Non-Wetting Phase
S_w	Saturation of Wetting Phase
a_{wn}	Interfacial Area
ρ_n	Density of Wetting Phase
μ_n	Viscosity of Non-Wetting Phase
p_d	Entry pressure in Brooks Corey
λ	Brooks-Corey Parameter
k_{rn}	Relative Permeability of Non-wetting phase
k_{rw}	Relative Permeability of wetting phase

S_{wr}	Residual Saturation of Wetting phase
q_{α}	Source term volume flux ($m^3/s \cdot m^3$)
\mathbf{g}	Gravity vector
p_w	Pressure of Wetting phase
p_n	Pressure of Non-wetting phase
p_c	Capillary pressure
Q_{in}	Injection Rate
$k_{n \rightarrow w}^R$	Reaction rate (k_{react})
v_w	Wetting phase velocity

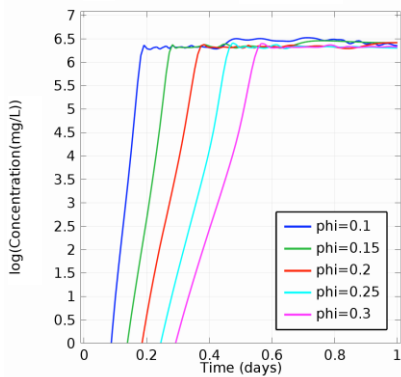


Figure 1. [Lab Scale Experiment] Tracer concentration BTCs for varying porosities at center of the domain.

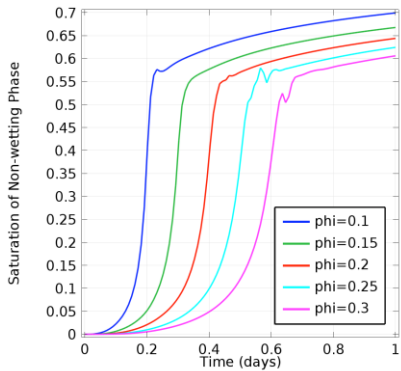


Figure 2. [Lab Scale Experiment] Non-wetting phase saturation BTCs for varying porosities at center of the domain

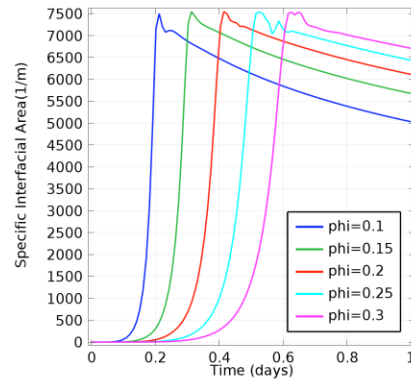


Figure 3. [Lab Scale Experiment] Specific interfacial area BTCs for varying porosities at center of the domain.

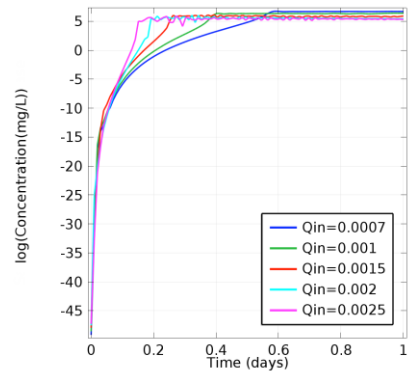


Figure 4. [Lab Scale Experiment] Tracer concentration BTCs on logarithmic scale for different injection rates at center of the domain

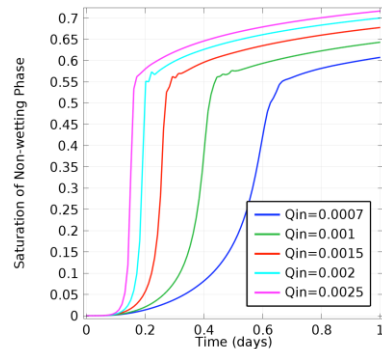


Figure 5. [Lab Scale Experiment] Non-wetting phase saturation BTCs for different injection rates at center of the domain

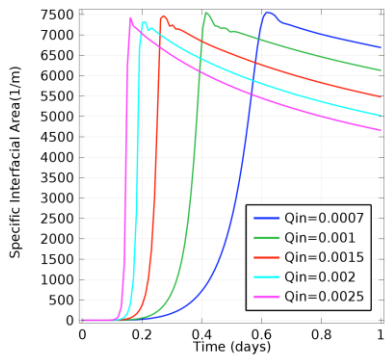


Figure 6. [Lab Scale Experiment] Specific interfacial area BTCs for different injection rates at center of the domain

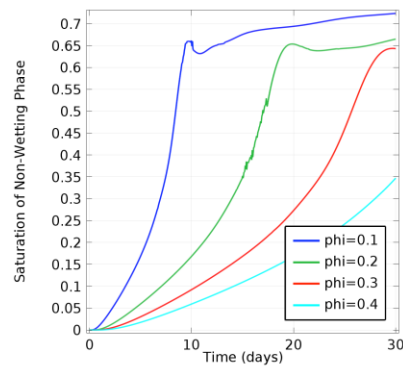


Figure 9. [Field Scale Experiment] Non-wetting phase saturation BTCs for varying Porosity values at 30 m from the injection well.

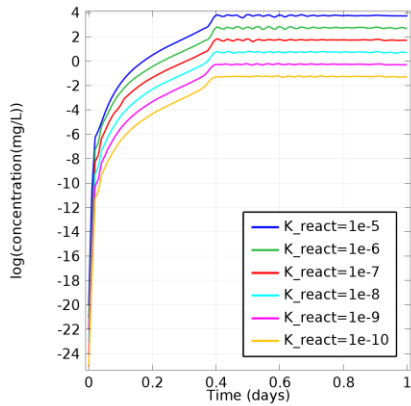


Figure 7. [Lab Scale Experiment] Tracer concentration BTCs for different reaction rates at center of the domain.

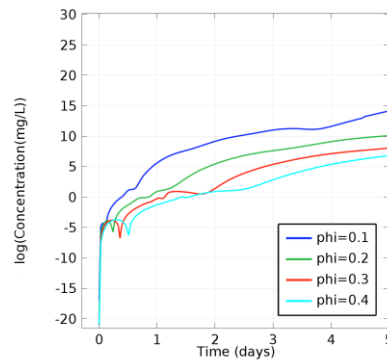


Figure 10. [Field Scale Experiment] Tracer concentration BTCs for varying Porosity values at 30 m from the injection well.

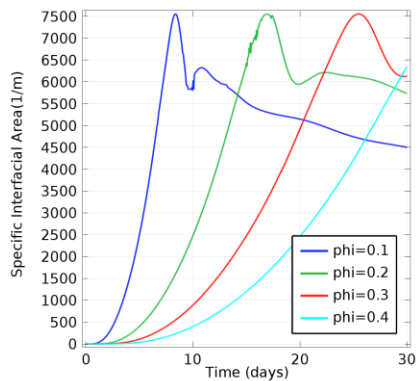


Figure 8. [Field Scale Experiment] Specific interfacial area BTCs for varying Porosity values at 30 m from the injection well.

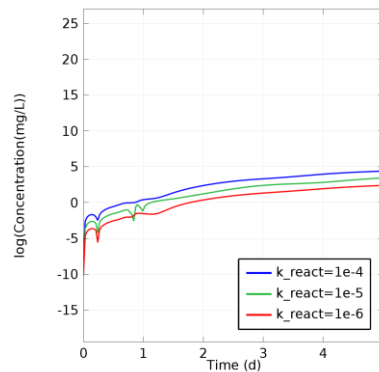


Figure 11. [Field Scale Experiment] Tracer concentration BTCs for different reaction rates at 30 m from the injection well.

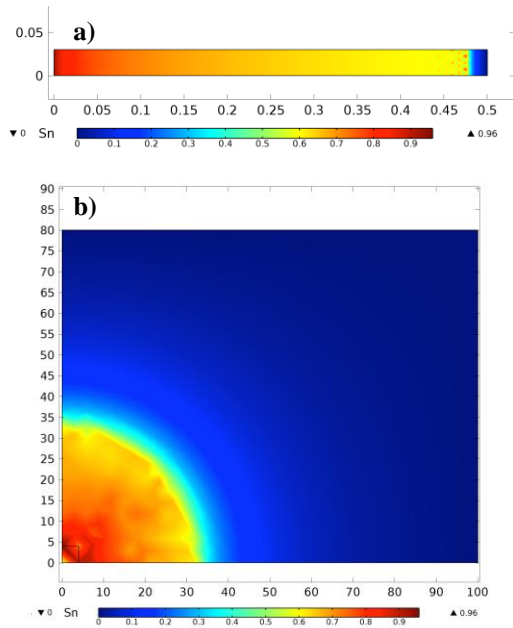


Figure 12. a) Laboratory scale experiment; b) Field Scale Experiment